ECS Journal of Solid State Science and Technology, **8** (11) P661-P666 (2019)
2162-8769/2019/8(11)/P661/6/$38.00 © The Electrochemical Society

Effects of Hydrogen Plasma Treatment Condition on Electrical Properties of β-Ga_2O_3

A. Y. Polyakov,[1] In-Hwan Lee,[2] N. B. Smirnov,[1] E. B. Yakimov,[1,3] I. V. Shchemerov,[1] A. V. Chernykh,[1] A. I. Kochkova,[1] A. A. Vasilev,[1] A. S. Shiko,[1] Patrick H. Carey IV,[4,*] F. Ren,[4,] and S. J. Pearton[5,**,z]**

[1]*National University of Science and Technology MISiS, Moscow 119049, Russia*
[2]*Department of Materials Science and Engineering, Korea University, Seoul 02841, Korea*
[3]*Institute of Microelectronics Technology and High Purity Materials, Russian Academy of Science, Chernogolovka, Moscow Region 142432, Russia*
[4]*Department of Chemical Engineering, University of Florida, Gainesville, Florida 32611, USA*
[5]*Department of Materials Science and Engineering, University of Florida, Gainesville, Florida 32611, USA*

The effects of hydrogen or deuterium plasma treatment at 330°C on electrical properties and deep trap spectra of n-type β-Ga_2O_3 films grown by halide vapor phase epitaxy on native n^+ substrates are reported. Under plasma treatment conditions giving rise to higher energy ions (280 eV), hydrogen penetrates into the HVPE films and fully compensates or passivates shallow donors to ∼2 μm from the surface. The Fermi level in this high-resistivity layer is pinned by electron traps near E_c-1 eV (E3 traps) also present in the starting material. Annealing at 450°C shifts the pinning position to another dominant deep trap in the starting material, the E2* traps near E_c-0.75 eV. Subsequent annealing at 550°C almost fully restores the electrical properties. By sharp contrast, plasma treatment under conditions of low energy ions (35eV) severely reduced hydrogen incorporation and only slightly increased the near-surface donor concentration. The observed differences are discussed under the assumption that hydrogen is introduced in the form of isolated acceptor interstitials with the charge transfer level near E_c-0.5 eV in the first case, but as a donor with level inside the conduction band in the second case as proposed by recent theoretical calculations.
© 2019 The Electrochemical Society. [DOI: 10.1149/2.0041911jss]

Manuscript submitted August 9, 2019; revised manuscript received October 14, 2019. Published October 23, 2019.

The behavior of dopants and impurities in β-Ga_2O_3 is of interest because of the growing importance of this ultra-wide bandgap material for next generation high-power devices and solar-blind photodetectors.[1–3] Hydrogen is among the impurities whose behavior needs to be understood since it is a common contaminant in many processes from growth by metallorganic chemical vapor phase epitaxy (MOVPE), halide vapor phase epitaxy (HVPE) to etching and cleaning with liquid solvents, dry etching in hydrogen-containing mixtures or with high temperature annealing.[4–7] In addition, hydrogen in other semiconductors has been shown to actively interact with defects and impurities, often rendering them electrically neutral (hydrogen passivation) and giving rise to beneficial effects, such as improved lifetime of charge carriers,[7] and also unwanted effects, such as passivation of intentionally introduced dopants. An example is the hydrogen passivation of Mg acceptors in III-Nitrides during MOVPE growth.[8]

Theory predicts for interstitial hydrogen H_i the charge transition level between the positively charged and negatively charged states, ε(+/−), to be close to E_c-0.51 eV,[9] while, for H_i captured by oxygen lone pairs (the most energetically favorable state,[6] the ε(+/−) level is located about 0.22 eV above the conduction band edge.[9,10] Thus, isolated hydrogen can behave either as a shallow donor in n-type material if introduced under equilibrium growth conditions, or as a relatively deep compensating acceptor when formed under highly nonequilibrium conditions. Hydrogen complexes with oxygen vacancies V_O can act as shallow donors,[6] form neutral complexes with deep Mg acceptors[7] and can interact with deep Ga vacancy acceptors changing their charge in relation to the number of hydrogen atoms in respective complexes.[8,9]

Experimental studies have mainly been done for hydrogen introduced by annealing at high temperature, with Local Vibrational Modes (LVM) spectroscopy indicating formation of hydrogen complexes with Mg acceptors,[11] and with V_{Ga} and V_O.[12,13] Annealing in H_2-free atmosphere removes such complexes and the release of "free" hydrogen in some cases resulted in stronger absorption by free carriers.[13,14] Hydrogen incorporation during high temperature annealing shows a strong anisotropy- incorporation is efficient for the (−201) orientation, but not for (010) orientation.[14] When hydrogen was introduced by by ion implantation, it can be detected by secondary ion spectrometry (SIMS) at depths corresponding to the ion range and concentrations determined by the ion fluence. Annealing at temperatures > 400°C results in hydrogen effusion from the samples.[15]

With proton implantation a strong decrease of the uncompensated donor density has been reported.[12,16–19] The implantation creates deep electron and hole traps,[17,18] but the aggregate densities of these traps, even assuming all are deep acceptors, is much lower than the electron removal rate. One explanation is formation of neutral complexes between the shallow donors and the vacancies produced by irradiation.[22] Another option[21,22] is that the observed phenomena could be related to the action of the ε (+/−) H_i acceptor state near E_c-0.52 eV.[9,19]

With exposure to a high ion energy plasma, deuterium is observed to penetrate deep into (−201) bulk Ga_2O_3 forming characteristic plateaus whose extent increased with treatment temperature from about 0.1 μm (100°C for 0.5 h) to about 0.7 μm (270°C)[15] as shown in Fig. 1a for the 270°C and 200°C profiles. The plateaus are usually associated with hydrogen/deuterium forming complexes with donors. Annealing at 400°C led to strong outdiffusion of hydrogen was almost complete after annealing at 500°C[15] (Fig. 1b). Hydrogen plasma treatment under similar plasma conditions at 330°C led to the top ∼2 μm of the treated n-type Ga_2O_3 rendered highly resistive, with the Fermi level pinned by dominant deep traps.[21] Annealing to 550°C essentially restored the initial properties.[21] With the high ion energy plasma conditions[5,21] one expects a high density of defects to be formed near the surface, as demonstrated in the cases of BCl_3 or Ar plasma induced damage.[22,23] In this paper, we demonstrate that the plasma conditions have a strong effect on hydrogen incorporation depth and concentration and under some conditions, little hydrogen penetration into the sample actually takes place. This suggests the hydrogen must overcome trapping at defects and self-trapping to form molecules in order to penetrate into the Ga_2O_3.

Experimental

The samples were from Tamura Corp/Novel Crystals Technologies (Japan) and were prepared by HVPE on top of bulk β-Ga_2O_3 substrates grown by edge-defined film-fed growth (EFG)[24] (the growth was done by the manufacturer) The film orientation was (010), with thickness ∼10 μm and were doped with Si to net shallow donor concentration of (1-2) × 10^{17} cm^{-3}. The substrates were doped with

*Electrochemical Society Student Member.
**Electrochemical Society Fellow.
zE-mail: spear@mse.ufl.edu

Downloaded on 2019-10-24 to IP 128.227.131.209 address. Redistribution subject to ECS terms of use (see ecsdl.org/site/terms_use) unless CC License in place (see abstract).

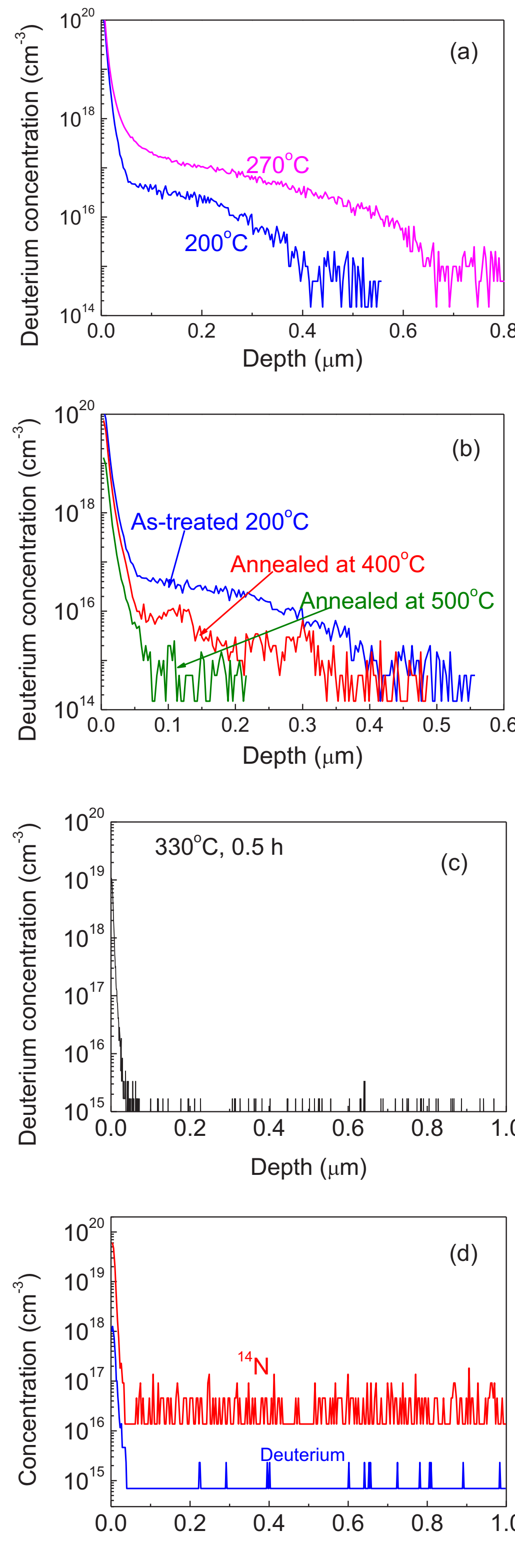

Figure 1. (a) Deuterium concentration profiles measured at two temperatures for treatments under harsh plasma conditions; (b) Deuterium concentration profiles after treatment at 200°C under harsh plasma conditions and annealed in nitrogen at 400°C and 500°C; (c) deuterium concentration profile for deuterium plasma treatment under mild plasma conditions; (d) ^{14}N and deuterium profiles after treatment in $^{14}ND_3$ plasma under mild plasma conditions.

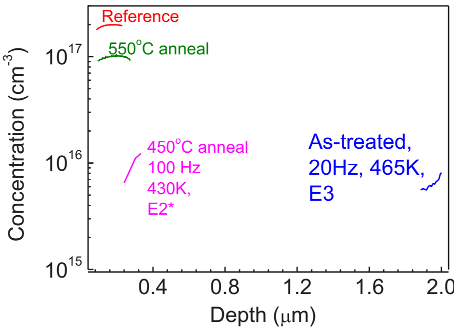

Figure 2. Room temperature concentration profiles from C-V measurements for the reference sample and sample after hydrogen plasma treatment and 550°C anneal; also shown are C-V concentration profiles obtained for the sample treated in hydrogen plasma and measured at 465K with probing frequency 20 Hz (this is the E3 center's concentration profile) and for the sample annealed at 450°C and measured at 100 Hz at 430K.

Sn to net donor concentration of 3×10^{18} cm^{-3}. Full-area back o contacts were prepared by electron beam deposition of Ti/Au on the Ar-plasma treated back surface. After the metal deposition, rapid thermal annealing at 300°C was performed to decrease the contact resistance. This back o contact annealing was performed prior to treatment in different plasma sources described below. After the plasma treatments, Ni/Au Schottky contacts about 1 mm in diameter were deposited at room temperature using E-beam evaporation.[16,22,23] Naturally, all measurements reported below, refer to the HVPE films, not to the EFG substrates.

Plasma treatments were performed in inductively coupled plasma (ICP) Plasma Therm Versaline reactor (USA) with ICP source frequency 2 MHz and power 400W. The RF frequency applied to the chuck was 13.56 MHz, with the chuck power 200W. The average ion energy incident on the samples is ~280 eV. The pressure was 0.5 Torr The source power controls the ion density in the plasma, while the chuck power determines the energy of ions in plasma. Two regimes were used-in the first, labelled "harsh", the chuck power was 200W. This regime was used for doing hydrogen plasma treatment at 330°C for 1 h and was previously used by us for deuterium diffusion studies which resulted in deuterium profiles depicted in Figs. 1a, 1b.[15] We call this regime harsh because it is similar to regimes used for dry etching of β-Ga_2O_3 known to produce near-surface damage due to bombardment with energetic ions in plasma.[22,23] No discernable etching was observed under our conditions.

The second regime used RF power of 30W, labelled "mild" because it does not give rise to rapid etch rates and does not change the electrical properties during dry etching.[23] The average ion energy under these conditions is ~35 eV. This regime was used to try to introduce at 330°C (0.5 h) deuterium, or ammonia, the latter in the form of $^{14}ND_3$ to facilitate SIMS profiling.

The samples were characterized before and after plasma exposures by capacitance-voltage C-V profiling, current-voltage I-V measurements, admittance spectra (AS) and deep level transient spectroscopy (DLTS).[25] In addition, because the sample treated in hydrogen under harsh conditions showed high resistivity in the surface region, it was characterized by photoinduced current transient spectroscopy (PICTS)[26] and current DLTS (CDLTS).[27–29]

Results and Discussion

Harsh hydrogen plasma treatments of the (010) n-Ga_2O_3 films treated at 330°C for 1 h showed a reduction in carrier density (Figure 2). In the as-hydrogenated sample, the capacitance was much lower than in the virgin sample and, at 25°C, did not depend on frequency or voltage, suggesting the top ~2 μm of the sample behaved effectively as a dielectric. This was confirmed by the low current for both bias polarities at 300K. Above 125°C, the capacitance below

Downloaded on 2019-10-24 to IP 128.227.131.209 address. Redistribution subject to ECS terms of use (see ecsdl.org/site/terms_use) unless CC License in place (see abstract).

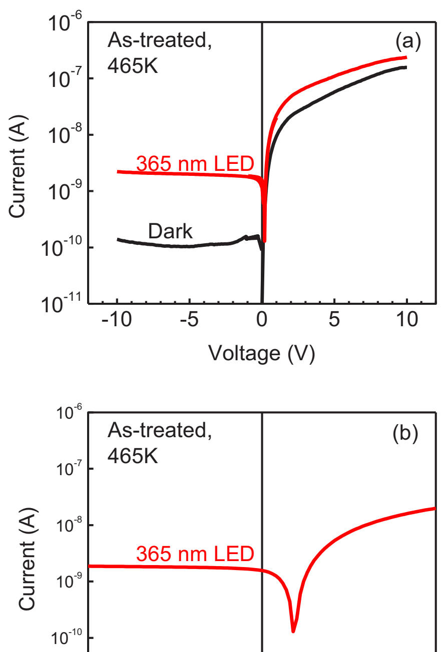

Figure 3. (a) 465K I-V characteristics measured in the dark and under 365 nm wavelength LED excitation for the sample treated in hydrogen plasma; (b) the blow-up of the low voltage region of the I-V characteristic measured under illumination.

100 Hz started to increase with temperature and formed a clear step at low frequencies, with the AC conductance G normalized by the angular frequency ω, G/ω[25] showing well defined peaks, with the peak position shifting to higher temperature with increasing frequency.[25] The dark I-V characteristics at these high temperatures showed features of a Schottky diode made on high resistivity n-type semiconductor (Fig. 3a): the current at positive voltage on the Schottky diode metal much higher than with negative bias, pronounced photocurrent with positive open circuit voltage V_{OC} (as seen in the blow-up of the light I-V characteristic in Fig. 3b). The dark current in the forward direction is low because of the series resistance of the highly resistive portion of the film (series resistance of 6×10^7 Ω at 180°C) and illumination increased the forward current, which is the consequence of the high resistivity of the top portion of the hydrogenated film.

A step in capacitance/peak in conductance is observed in AS spectra when the Fermi level crosses a level in the bandgap.[25] As we know that our material after hydrogen treatment is high-resistivity n-type the level we observe in AS spectra should be located in the upper half of the bandgap and should be the one pinning the Fermi level. Standard AS analysis based on measurements of the step/peak temperature with the probing signal frequency[25] gives the position of the level responsible for the peak in admittance as E_c-1.05 eV with electron capture cross section of 2×10^{-13} cm^2. The profiles shown after plasma treatment were determined from C-V measurements at low frequency and high temperature at which the step appeared in capacitance versus frequency in AS spectra. This step signifies that the Fermi level crosses the level of the deep trap, while the energy of the trap is determined from AS analysis. The signature of this center coincides with the signature of one of the two dominant electron traps detected in DLTS spectra of the virgin sample, the E3 defect.[17,30] In high resistivity n-type material with the Fermi level pinned by a deep center near E_c-1.05 eV, the extent of the space charge region and the capacitance

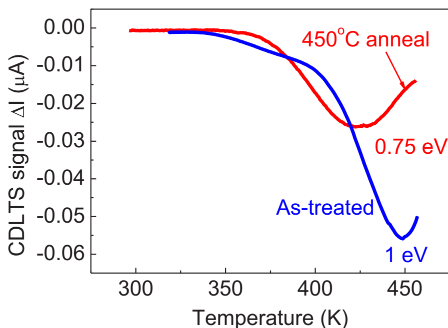

Figure 4. CDLTS spectra measured after the hydrogen plasma treatment and after subsequent anneal at 450°C, measurements at −10 V, with pulsing to +5V for 3s, time windows 8 ms/ 80 ms.

at low frequency are determined by the number of electrons residing on the trap.[28]

C-V measurements at high temperature and low frequency allow calculation of the concentration of electrons on this level as a function of depth.[28] From Fig. 2 showing the results of C-V profiling at 20 Hz and 180°C the density of electrons on this center near E_c-1.05 eV is 7×10^{15} cm^{-3} at 2 μm from the surface. The concentration of the center determined for the virgin sample from DLTS was 1.7×10^{15} cm^{-3}.[29] PICTS spectra measurements on this sample with excitation provided by pulses of illumination with 3.4 eV photons were dominated by the 1.05 eV centers.[21] As seen in Fig. 3, the hydrogenated film showed an appreciable forward current at elevated temperatures, allowing measurement of the deep trap spectra with CDLTS.[25]

Fig. 4 shows a spectrum measured with constant bias of −10V and forward bias pulse of +5V (3-s-long, the spectrum was obtained with time windows $t_1/t_2 = 8$ ms/ 80 ms). Standard CDLTS analysis yielded an activation energy of 1 eV, close to that of the E3 centers. Thus we observe that after hydrogen plasma treatment in harsh conditions the top ∼2 μm is heavily compensated and highly resistive and the Fermi level is pinned by the E3 electron traps also present in the starting conditions. The concentration is higher than before treatment.

RTA for 5 min in N_2 resulted in the thickness of the high resistivity portion of the film becoming lower and the temperature at which the step was observed in capacitance moving to lower temperature. Admittance spectra measured in the low frequency/high temperature region yielded the center pinning the Fermi level as 0.75 eV, with electron capture cross section 1.2×10^{-15} cm^2.[21] The concentration profile calculated from C-V measurements at 160°C and 100 Hz and giving the concentration of uncompensated 0.75 eV centers is shown in Fig. 2. This concentration was $\sim 10^{16}$ cm^{-3} at 0.3 μm from the surface. CDLTS spectra were dominated by a trap at E_c-0.75 eV (Fig. 4). The parameters of this center are similar to those of the second dominant electron trap in the virgin sample, the E2* trap[17,21] with density 5.4×10^{15} cm^{-3} before the hydrogen plasma treatment.[21] Further annealing at 550°C restored the starting density of uncompensated shallow donors (Fig. 2) and the initial concentrations of the E2* and E3 deep electron traps.[21]

For hydrogen plasma treatment under the harsh conditions, the top ∼2 μm of the sample becomes highly resistive, with the Fermi level pinned by the E3 centers whose concentration is higher than before treatment. The density of these traps, even if they are acceptors, is not sufficiently high to compensate the 2×10^{17} cm^{-3} shallow donors present before hydrogenation. There is the possibility that plasma damage creates deep compensating centers, but previous studies on samples treated in Ar plasma under similar conditions show that a) the width of the damaged region is confined to the top ∼0.2 μm of the sample and b) the density of deep traps created can affect the voltage offset in C-V measurements, decreasing it due to additional deep traps near the surface, but not to totally compensate the shallow donors.[21] The depth to which the shallow donors are compensated/passivated

Downloaded on 2019-10-24 to IP 128.227.131.209 address. Redistribution subject to ECS terms of use (see ecsdl.org/site/terms_use) unless CC License in place (see abstract).

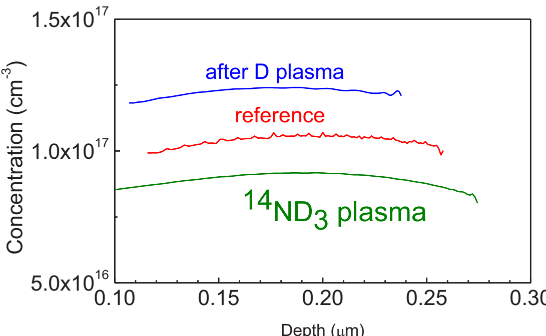

Figure 5. Room temperature CV profiles measured before exposure to deuterium and $^{14}ND_3$ plasma (reference sample) and after such exposure.

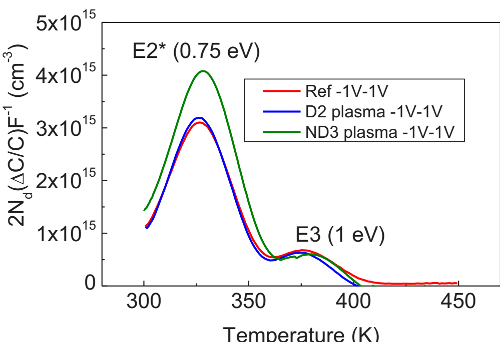

Figure 7. DLTS spectra of the sample before plasma exposure and samples after exposure to deuterium and 14ND$_3$ plasmas, the spectra shown for applied bias −1V, bias pulse to 1 V (3s-long), time windows 1.35 s/ 13.5 s.

under the harsh hydrogen plasma treatment conditions (330°C, 1 h) is of the right order of magnitude expected from previous SIMS profiling experiments performed using this plasma source (illustrated in Fig. 1a) if one takes into account the higher temperature of treatment (330°C instead of 270°C), the longer treatment time (1 h compared to 0.5 h), and the use of hydrogen instead of deuterium.[15,21] It appears hydrogen is either compensating existing shallow donors if it diffuses in the H_i^- form (charge transfer level near E_c-0.5 eV[9] or forming neutral complexes with them (passivating them) as is common for many other semiconductors.[4–7] The change of the width of the passivated region and the compensation /passivation ratio of shallow donors with annealing at 450°C and 550°C is in general agreement with the results of SIMS profiling of Fig. 1b.[17]

The results of hydrogen plasma treatment under mild conditions were radically different. Fig. 1c shows that deuterium does not penetrate into the sample treated under these conditions, even though the temperature and the treatment time were the same. As seen in Fig. 5, we also observed no change in concentration profiles after the deuterium plasma treatment, rather the density of shallow donors was increased after the treatment. The I-V characteristics also were not strongly affected; the ideality factor was equal to 1, the series resistance and the saturation current density in the forward direction were similar. The reverse current was higher in the reference sample before the deuterium treatment and the reverse current increased more rapidly at high voltages in the reference sample (see Fig. 6). DLTS spectra showed little change after deuterium plasma treatment, as illustrated by Fig. 7 comparing the spectra for the near-surface region probed with reverse bias −1V and forward bias pulse of 1V. These spectra were dominated by E2* electron traps near E_c-0.75 eV and E3 traps near E_c-1.05 eV in lower concentration.

To explain this difference in behavior of hydrogen/deuterium when introduced from harsh and from mild plasma one might consider that, in the former case, the ions in plasma have relatively high energy and create damage at the near surface region that could facilitate hydrogen

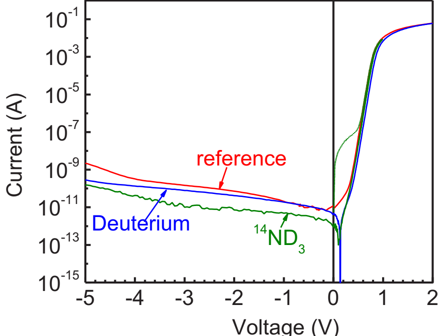

Figure 6. Room temperature I-V characteristics of the samples before plasma exposure and after exposure to deuterium plasma and to $^{14}ND_3$ plasma.

to be introduced in the form of non equilibrium isolated interstitial acceptors H_i^-,[9,10] similar to the case of hydrogen introduced by ion implantation.[17] With mild plasma treatment, hydrogen can be incorporated in the more thermodynamically stable form of donors with level ∼0.2 eV within the conduction band.[9,10] If the isolated H acceptors have higher diffusivity that could explain stronger effects under the harsh plasma: deep H penetration into the sample, compensation or passivation of shallow donors, whereas, for mild hydrogen plasma treatment one observes the enhancement of shallow donors concentration due to hydrogen donors, as observed in n-ZnO.[31] When calculating the charge transition levels from the dependence of the defect formation energy on the Fermi level position the theorists naturally consider the defects configurations that are lowest in energy. Such defects will dominate under equilibrium conditions. For hydrogen interstitials these low formation energy defects are expected to have the ε(+/−) charge transfer level high inside the conduction band as described in Ref. 10. These are hydrogen states observed under conditions close to equilibrium, such as when hydrogen is introduced from hydrogen gas by high temperature annealing or when it is introduced from hydrogen plasma which does not cause surface damage. However, the authors of Ref. 9 found that there exist other H_i configurations with a higher formation energy that that have the ε(+/−) charge transition level inside the bandgap at about E_c-0.5 eV. Such interstitials will not form under equilibrium conditions, but will form when the conditions are very far from equilibrium, as in harsh hydrogen plasma treatment.

It was interesting to compare plasma treatment effects for mild plasma conditions when the donor-promoting hydrogen/deuterium was combined with a presumably compensating agent, such as nitrogen.[32,33] This was done by using a plasma of $^{14}ND_3$ isotopes to facilitate SIMS profiling. These treatments were done under the same conditions as in the mild deuterium plasma treatment. SIMS profiles measured after the treatment (Fig. 1d) showed that both elements were below the SIMS sensitivity limit everywhere but at the immediate surface. However, C-V profiling (Fig. 5) indicated the net donor concentration after the $^{14}ND_3$ treatment was lower than for the reference and deuterium treated samples. This was accompanied by the decrease of the voltage intercept in $1/C^2$ versus V plots for the $^{14}ND_3$ treated sample to 1.15 V compared to 1.25-1.3 V in the reference and D-treated samples. Moreover, we observed a measurable decrease of reverse current and increase of the near-surface concentration of the E2* electron traps after the $^{14}ND_3$ treatment (Figs. 6 and 7). We can tentatively associate the decrease in the surface concentration, in the voltage intercept in C-V and the decrease in reverse current with the presence of near surface layer with a higher density of deep traps due to nitrogen concentration tail extending into the sample but not detectable by SIMS. This could promote increased density of deep traps in the surface region and result in lower voltage intercept in C-V,[22] lower net donor concentration, and lower reverse current.

Downloaded on 2019-10-24 to IP 128.227.131.209 address. Redistribution subject to ECS terms of use (see ecsdl.org/site/terms_use) unless CC License in place (see abstract).

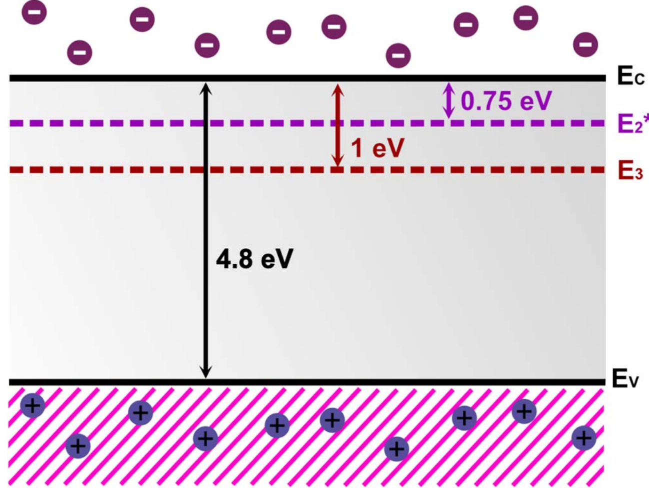

Figure 8. Summary of defect levels observed in the bandgap as a result of plasma exposure.

Figure 8 summarizes the observed levels produced in the gap by plasma exposure.

Conclusions

When treated in hydrogen or deuterium plasmas characterized by relatively high energy of ions in the plasma causing substantial plasma damage in the near-surface region, hydrogen/deuterium can propagate deep into Ga_2O_3, demonstrating a characteristic plateau in concentration whose extent increases with increasing treatment temperature. Electrical properties of these samples are strongly affected down to the depth similar to the expected hydrogen penetration depth, about 2 μm for the treatment temperature and time of 330°C, 1h. In this region, all shallow donors are passivated or compensated so the Fermi level is pinned by deep electron traps already present before H plasma treatment, the E3 traps with level E_c-1.05 eV. The concentration of these traps is higher than before hydrogen treatment, suggesting that defects could be complexes involving hydrogen. In the starting samples, the dominant electron traps were E2* defects with levels E_c-0.75 eV, with E3 trap concentration being half an order of magnitude lower, no signal related to E2* centers could be observed in hydrogen treated samples. The effects of annealing suggest a close relation between the presence of hydrogen and the changes in electrical properties and in deep trap spectra of the hydrogen treated samples.

When deuterium is introduced from the plasma in which the energy of the bombarding ions is much lower, causing less near-surface damage, the deuterium penetration was negligible, and the only effects were a slight increase in the near-surface density of shallow donors and decrease of the reverse leakage current. The observed differences in hydrogen penetration and behavior could be attributed to the difference in energies of H ions impinging the surface of the samples. When the energy is high, hydrogen can be introduced as an isolated H_i^- acceptor species with the charge transfer ε(+/−) level near E_c-0.5 eV.[9] Hydrogen/deuterium introduced that way is mobile,[12,19] and can compensate shallow donors or passivate them, forming neutral complexes. The strong compensation of n-type conductivity in proton irradiated n-Ga_2O_3 has been ascribed to the action of such hydrogen species.[12,19] With low hydrogen ion energy, the conditions are closer to equilibrium and the dominant species is the H_i captured by lone O pairs that is a donor with level about 0.2 eV deep within the conduction band.[9,10] Such hydrogen would be less mobile in n-type Ga_2O_3 and will not contribute to shallow donor compensation/passivation, but can increase near-surface shallow donor density. When hydrogen incorporation into Ga_2O_3 was achieved by high temperature anneals in hydrogen/deuterium, an anisotropy has been detected, with hydrogen readily going in for (−201) orientation, but not for (010) orientation.[14] However, with that mode of hydrogen introduction, the dominant species should always be the E_c+0.2 eV H_i donors. The deuterium profiles in Fig. 1a were obtained for (−201) orientation whereas the passivation studies described by Figs. 2–4 were obtained on (010) oriented HVPE, yet the data are consistent with hydrogen incorporating several microns and interacting with shallow donors.

Acknowledgments

The work at NUST MISiS was supported in part by the Russian Science Foundation, grant no. 19-19-00409. The work at UF was sponsored by the Department of the Defense, Defense Threat Reduction Agency, HDTRA1-17-1-011, monitored by Jacob Calkins and also by NSF DMR 1856662 (Tania Paskova).

ORCID

A. Y. Polyakov https://orcid.org/0000-0001-6898-6126
In-Hwan Lee https://orcid.org/0000-0003-4566-9181
N. B. Smirnov https://orcid.org/0000-0002-4993-0175
A. V. Chernykh https://orcid.org/0000-0003-2450-8872
Patrick H. Carey IV https://orcid.org/0000-0002-8826-3977
S. J. Pearton https://orcid.org/0000-0001-6498-1256

References

1. H. von Wenckstern, *Adv. Electron Mater*, **3**, 1600350 (2017).
2. S. J. Pearton, Jiancheng Yang, Patrick H. Cary, F. Ren, Jihyun Kim, Marko J. Tadjer, and Michael A. Mastro, *Appl. Phys. Rev.*, **5**, 011301 (2018).
3. Michael A. Mastro, Akito Kuramata, Jacob Calkins, Jihyun Kim, Fan Ren, and S. J. Pearton, *ECS J. Solid State Sci. Technol.*, **6**. P356 (2017).
4. M. Stavola, *AIP Conference Proceedings*, **671**, 21 (2003).
5. M. Stavola and W. B. Fowler, *J. Appl. Phys.*, **123**, 161561 (2018).
6. M. Stavola, *Materials Science Forum*, **148**, 251 (1994).
7. S. J. Pearton, J. W. Corbett, and T. S. Shi, *Appl. Phys. A*, **43**, 153(1987).
8. S. Nakamura, *Angew. Chem., Int. Ed.*, **54**, 7770 (2015).
9. J. E. N. Swallow, J. B. Varley, L. A. H. Jones, J. T. Gibbon, L. F. J. Piper, V. R. Dhanak, and T. D. Veal, *APL Mater.*, **7**, 022528 (2019).
10. J. B. Varley, J. R. Weber, A. Janotti, and C. G. Van de Walle, *Appl. Phys. Lett.*, **97**, 142106 (2010).
11. Jacob R. Ritter, Jesse Huso, Peter T. Dickens, Joel B. Varley, Kelvin G. Lynn, and Matthew D. McCluskey, *Appl. Phys. Lett.*, **113**, 052101 (2018).
12. M. E. Ingebrigtsen, A. Yu. Kuznetsov, B. G. Svensson, G. Alfieri, A. Mihaila, U. Badstubner, A. Perron, L. Vines, and J. B. Varley, *APL Mater.*, **7**, 022510 (2019).
13. Ying Qin, Michael Stavola, W. Beall Fowler, Philip Weiser, and S. J. Pearton, *ECS J. Solid State Sci. Technol.*, **8**, Q3103 (2019).
14. Michael Stavola, W. Beall Fowler, Ying Qin, P. Weiser, and Stephen J. Pearton, Thermal Stabilities of Hydrogen-Related Defects in Ga_2O_3, *ICDS* 2019.
15. Ribhu Sharma, Erin Patrick, and E Mark, Law, Shihyun Ahn, F. Ren, S. J. Pearton, and A. Kuramata, *ECS J. Solid State Sci. Technol.*, **6**, P794 (2017).
16. A. Y. Polyakov, N. B. Smirnov, I. V. Shchemerov, E. B. Yakimov, Jiancheng Yang, F. Ren, Gwangseok Yang, Jihyun Kim, A. Kuramata, and S. J. Pearton, *Appl. Phys. Lett.*, **112**, 032107 (2018).
17. M. E. Ingebrigtsen, J. B. Varley, A. Yu. Kuznetsov, B. G. Svensson, G. Alfieri, A. Mihaila, U. Badstübner, and L. Vines, *Appl. Phys. Lett.*, **112**, 042104 (2018).
18. A. Y. Polyakov, N. B. Smirnov, I. V. Shchemerov, E. B. Yakimov, S. J. Pearton, Chaker Fares, Jiancheng Yang, Fan Ren, Jihyun Kim, P. B. Lagov, V. S. Stolbunov, and A. Kochkova, *Appl. Phys. Lett.*, **113**, 092102 (2018).
19. J. B. Varley, M. E. Ingebrigtsen, A. Yu. Kuznetsov, B. G. Svensson, G. Alfieri, A. Mihaila, U. Badstubner, V. Lordi, A. Perron, and L. Vines, Theoretical and experimental assessments of deep level defects in proton irradiated β-Ga_2O_3, *ICDS* 2019.
20. L. Vines, C. Bhoodoo, H. von Wenckstern, and M. Grundmann, *J. Phys.: Condens. Matter*, **30**, 025502 (2018).
21. A. Y. Polyakov, In-Hwan Lee, N. B. Smirnov, E. B. Yakimov, I. V. Shchemerov, A. V. Chernykh, A. I. Kochkova, A. A. Vasilev, F. Ren, P. H. Carey, and S. J. Pearton, *Appl. Phys. Lett.*, **115**, 032101 (2019).
22. A. Y. Polyakov, In-Hwan Lee, N. B. Smirnov, E. B. Yakimov, I. V. Shchemerov, A. V. Chernykh, A. I. Kochkova, A. A. Vasilev, P. H. Carey, F. Ren, David J. Smith, and S. J. Pearton, *APL Mater.*, **7**, 061102 (2019).
23. Jiancheng Yang, Shihyun Ahn, F. Ren, Rohit Khanna, Kristen Bevlin, Dwarakanath Geerpuram, S. J. Pearton, and A. Kuramata, *Appl. Phys. Lett.*, **110**, 142101 (2017).
24. www.tamura-ss.co.jp/en/products
25. *Capacitance spectroscopy of semiconductors*, ed. V. Jian, Li, and Giorgio Ferrari, (Pan Stanford Publishing Pte Ltd, Singapore, 2018) 437 pp.
26. M. Tapiero, N. Benjelloun, J. P. Zielinger, S. El Hamd, and C. Noguet, *J. Appl. Phys.*, **54**, 4006 (1988).

Downloaded on 2019-10-24 to IP 128.227.131.209 address. Redistribution subject to ECS terms of use (see ecsdl.org/site/terms_use) unless CC License in place (see abstract).

27. Alexander Y. Polyakov, Nikolai B. Smirnov, In-Hwan Lee, and Stephen J. Pearton, *J. Vac. Sci. Technol. B*, **33**, 061203 (2015).
28. A. Y. Polyakov, N. B. Smirnov, I. V. Schemerov, A. V. Chernykh, E. B. Yakimov, A. I. Kochkova, A. N. Tereshchenko, and S. J. Pearton, *ECS J. Solid State Sci. Technol*, **8**, Q3091 (2019).
29. A. Y. Polyakov, N. B. Smirnov, I. V. Shchemerov, E. B Yakimov, S. J. Pearton, Fan Ren, A. V. Chernykh, D. Gogova, and A. I. Kochkova, *ECS J. Solid State Sci. Technol*, **8**, Q3019 (2019).
30. K. Irmscher, Z. Galazka, M. Pietsch, R. Uecker, and R. Fornari, *J. Appl. Phys.*, **110**, 063720 (2011).
31. A. Y. Polyakov, N. B. Smirnov, A. V. Govorkov, K. Ip, M. E. Overberg, J. W. Heo, D. P. Norton, S. J. Pearton, B. Luo, F. Ren, and J. M. Zavada, *J. Appl. Phys.*, **94**, 400 (2003).
32. H. Peelaers and C. G. de Walle, *APL Mat*, **7**, 022519 (2019).
33. Kornelius Tetzner, Andreas Thies, Eldad Bahat Treidel, Frank Brunner, Günter Wagner, and Joachim Würfl, *Appl. Phys. Lett.*, **113**, 172104 (2018).

Downloaded on 2019-10-24 to IP **128.227.131.209** address. Redistribution subject to ECS terms of use (see **ecsdl.org/site/terms_use**) unless CC License in place (see abstract).